PHYSICAL REVIEW E, VOLUME 65, 030802(R)

Phase diagram of a mixed polymer brush

M. Müller
Institut für Physik, WA 331, Johannes Gutenberg Universität, D-55099 Mainz, Germany
(Received 25 October 2001; published 12 February 2002)

We investigate the structure and phase behavior of a two-component (binary) polymer brush in a solvent within self-consistent field theory as a function of the chains' stretching, the composition, and the incompatibility. Grafting the chains irreversibly prevents macrophase separation and the chains assemble into three-dimensional structures with lateral periodicity. At small incompatibilities a ''ripple'' phase is formed where different species aggregate into an array of parallel cylinders. At larger incompatibilities or asymmetric composition two ''dimple'' phases become stable, where different species form clusters which arrange on a quadratic (checkerboard structure) or hexagonal lattice.

DOI: 10.1103/PhysRevE.65.030802 PACS number(s): 61.25.Hq, 61.46.+w, 05.70.Np

The grafting of polymers to surfaces is an efficient means of tailoring surface properties. Polymer brushes find widely spread applications ranging from colloidal stabilization and tribology to biocompatibility. Recent experiments [1] have explored the properties of binary brushes which consist of hydrophilic and hydrophobic homopolymers. If the binary brush is in contact with a hydrophilic solvent the hydrophilic constituent segregates to the surface and *vice versa*. The segregation is reversible and provides a technique to tune the wetability of the coated surface.

The details of the local organization of the chains in the binary brush are, however, not known. Besides segregation perpendicular to the surface laterally structured phases might become stable [2]. Even a single-component brush in a bad solvent does not collapse into a uniform dense layer [3], but forms dimples, i.e., small clusters on the surface which are separated by a distance of the chain extension. Binary systems exhibit a rich behavior: Singh and co-workers [4] have studied a binary brush in the limit of low-grafting densities. If the solvent is bad for one component and good for the other component surface micelles form, i.e., the component with the low-solvent affinity collapses into a dense core, which is shielded by the other component. The self-assembled structures have been explored by scaling considerations and illustrated by two-dimensional (2D) self-consistent field (SCF) calculations. Marko and Witten [2] studied the onset of phase separation for very high-grafting densities. Under melt conditions the phase separation occurs laterally, i.e., rather than segregating to the top or the bottom of the brush the components A and B demix laterally and form ''ripples.'' Simulations [5–7] give evidence for lateral phase separation. Under bad solvent conditions the occurrence of more complex structures has been exemplified [5]. The thermodynamic stability of the structures, however, could not be addressed and the phase diagram is unknown.

Binary brushes might offer an alternative for producing patterned surfaces [8–11] and provide a model system for studying molecular self-assembly. We outline a general 3D self-consistent field theory (SCFT) to investigate the self-assembled structures of a binary brush with quenched grafting points and find three 3D structures with lateral periodicity.

We consider a binary polymer brush in a volume $V_0 = \Delta_0 L L$. L is the lateral extension of the brush, while Δ_0 denotes the extension perpendicular to the grafting surface. The brush contains $n = \sigma L^2$ polymers. Both polymer species—A and B—contain the same number of monomeric units N and are modeled as Gaussian chains of end-to-end distance R_e. Since the grafted ends are immobile, we identify each chain by its grafting position $\mathbf{r}_0$ and treat each grafted chain formally as an individual component.

We expand the interaction energy E in terms of the monomer densities ϕ_A and ϕ_B and retain only second virial coefficients

$$\frac{E[\phi_A,\phi_B]}{kT} = \int \mathrm{d}\mathbf{r}\left\{\frac{v_{AA}}{2}\phi_A^2 + \frac{v_{BB}}{2}\phi_B^2 + v_{AB}\phi_A\phi_B\right\}. \quad (1)$$

Our calculations are limited to solvents of good and marginal quality [12]. $v = (v_{AA}+v_{BB}+2v_{AB})/4$ characterizes the average strength of the excluded volume interaction between monomers. $\tilde{\chi} = (2v_{AB}-v_{AA}-v_{BB})/2v$ denotes the mutual attraction (repulsion) between (un)like monomers. It is related to the commonly used Flory-Huggins parameter via $\chi_{FH} = v\tilde{\chi}$. Increasing $\tilde{\chi}$ we increase the incompatibility between the two species and reduce the solvent quality. $\zeta = (v_{AA}-v_{BB})/2v$ specifies the solvent selectivity towards the A and B species. In the following we assume that the solvent is nonselective ($\zeta = 0$).

We employ SCFT to calculate the structure and phase behavior of the system of infinitely many chains with quenched grafting points $\mathbf{r}_0$ The free energy takes the form $F = E - T(S_A + S_B)$, where S_A and S_B are the conformational entropies of A polymers and B polymers, respectively. Within SCFT S_A is given by

$$S_A = k\sum_{A\mathbf{r}_0}\left\{\ln \mathcal{Q}_{A\mathbf{r}_0} + \int \mathrm{d}\mathbf{r}\, w_A \phi_{A\mathbf{r}_0}\right\}, \quad (2)$$

where $\mathcal{Q}_{A\mathbf{r}_0}[w_A]$ is the single-chain partition function of the A polymer, which is grafted at point $\mathbf{r}_0$, in an external field w_A. The sum runs over grafting points $\mathbf{r}_0$ for all A chains. $\phi_{A\mathbf{r}_0}$ denotes the monomer density of that A polymer. They satisfy the self-consistent set of equations

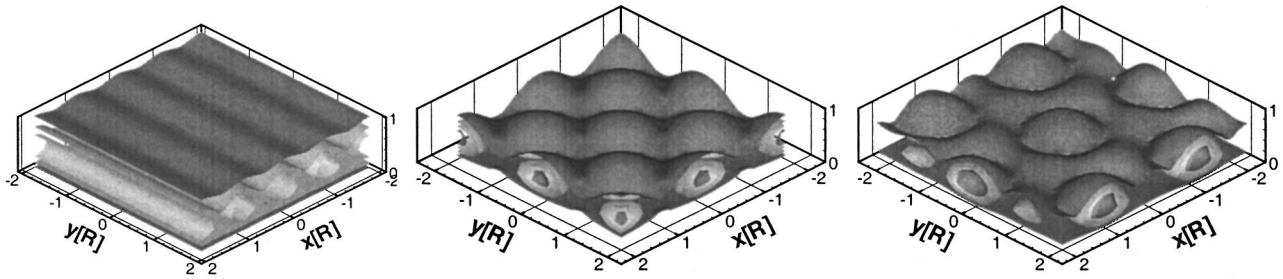

FIG. 1. Contours of the total density at $\Phi=1/2$ in the vicinity of the triple point. The segregated regions are more dense than regions where the *A* and *B* component mix. In the "ripple" phase (left) the species cluster into cylinders, every second one is rich in the *A* component. In the symmetrical "dimple *S*" phase (middle) *A* and *B* clusters alternate on a quadratic lattice. In the "dimple *A*" phase (right), the *A* component clusters and the dense regions form a hexagonal lattice, while the *B* component is collapsed and fills the space between the *A*-rich clusters.

$$w_A=\frac{\mathcal{D}E}{kT\mathcal{D}\phi_{A\mathbf{r}_0}}=v\left\{\frac{2-\tilde{\chi}}{2}\,\phi_A+\frac{2+\tilde{\chi}}{2}\,\phi_B\right\}$$

and

$$\phi_{A\mathbf{r}_0}=-\frac{1}{\mathcal{Q}_{A\mathbf{r}_0}}\frac{\mathcal{D}\mathcal{Q}_{A\mathbf{r}_0}}{\mathcal{D}w_A}. \tag{3}$$

The field w_A is independent from the grafting point $\mathbf{r}_0$. Similar expressions hold for S_B, w_B, and $\phi_{B\mathbf{r}_0}$.

To calculate the monomer density it is useful to define the end segment distributions $q_{A\mathbf{r}_0}(\mathbf{r},t)$ and $\tilde{q}_A(\mathbf{r},t)$. The former quantity denotes the spatial probability distribution of the end segment of a chain of length Nt which is grafted at $\mathbf{r}_0$, the latter refers to a free (i.e., not grafted) chain. Both end segment distributions satisfy the diffusion equation: $\partial q_A/\partial t=(R_e^2/6N)\Delta q_A-w_Aq_A$. One chain end is grafted at $\mathbf{r}=\mathbf{r}_0$ and, hence, $q_{A\mathbf{r}_0}(\mathbf{r},0)=\delta(\mathbf{r}-\mathbf{r}_0)$, while the other chain end is free $\tilde{q}_A(\mathbf{r},0)=1$. $\phi_{A\mathbf{r}_0}$ and $\mathcal{Q}_{A\mathbf{r}_0}$ can be expressed as

$$\phi_{A\mathbf{r}_0}(\mathbf{r})=\frac{1}{\mathcal{Q}_{A\mathbf{r}_0}}\int_0^N \mathrm{d}t\, q_{A\mathbf{r}_0}(\mathbf{r},t)\tilde{q}_A(\mathbf{r},N-t)$$

with

$$\mathcal{Q}_{A\mathbf{r}_0}=\int \mathrm{d}\mathbf{r}\, q_{A\mathbf{r}_0}(\mathbf{r},s)\tilde{q}_A(\mathbf{r},N-s)\quad \forall s. \tag{4}$$

We obtain the total *A* monomer density ϕ_A by summing over all grafting points of *A* chains

$$\phi_A(\mathbf{r})=\int_0^N \mathrm{d}t\, q_A(\mathbf{r},t)\tilde{q}_A(\mathbf{r},N-t), \tag{5}$$

with $q_A=\Sigma_{A\mathbf{r}_0}\, q_{A\mathbf{r}_0}/\mathcal{Q}_{A\mathbf{r}_0}$. Since q_A is a linear combination of $q_{A\mathbf{r}_0}$ it also obeys the diffusion equation with initial condition $q_A(\mathbf{r},0)=\Sigma_{A\mathbf{r}_0}\delta(\mathbf{r}-\mathbf{r}_0)/\tilde{q}_A(\mathbf{r}_0,N)$ where we have employed Eq. (4) with $s=0$. The density distribution of the 0th segment reproduces the grafting points: $\phi_A(\mathbf{r},t=0)=q_A(\mathbf{r},0)\tilde{q}_A(\mathbf{r},N)=\Sigma_{A\mathbf{r}_0}\delta(\mathbf{r}-\mathbf{r}_0)$.

In inhomogeneous systems we expand the spatial dependence of densities and fields in a set of orthonormal functions [14]. For periodic structures in the lateral direction, the free energy is minimized with respect to the unit-cell size *L*. Comparing the free energy of different spatial structures, we construct the phase diagram.

The equations above describe a binary brush with an arbitrary distribution of grafting points within SCF theory. At this stage, correlations and inhomogeneities of the grafting densities could be incorporated into the description. In the following, however, we assume that the grafting is laterally homogeneous and denote the relative concentration of *A* chains by Φ and replace the summation over the grafting points by an integral $\Sigma_{A\mathbf{r}_0}\to\Phi\sigma\int d\mathbf{r}_0\,\delta(x_0)$. Measuring the degree of stretching [13] by the dimensionless parameter $1/\delta^3=3/2[vN^2/R_e^3]^2[\sigma R_e^2]^2$ we define a rescaled *A* monomer density $\rho_A\equiv vN\delta\Phi\phi_A$ and measure all length scales in units of R_e. Within SCFT the chain length *N*, grafting density σ and the excluded volume strength v enter only via the combination δ.

Qualitative insight into the physical origin of phase separation can be gained in the limit of strong stretching $\delta\to 0$, where the situation is similar to the binary brush in the melt [2]. Then, the dominant contribution to the free energy stems from the interplay between excluded volume interactions and chain stretching (similar to the one-component brush). Using that the height of the brush scales like $h\sim R_e/\sqrt{\delta}$ this contribution is of the order kT/δ per chain. It controls the density profile. Upon increasing the incompatibility $\tilde{\chi}$, there is a transition from the disordered phase to the "ripple" phase as to reduce the energy of mixing. For $\delta\to 0$, only the composition $\rho_A-\rho_B$ becomes laterally inhomogeneous but not the total density $\rho_A+\rho_B$. The energy of mixing is of order $\tilde{\chi}kT/\delta$ per chain. Lateral demixing reduces the entropy of mixing of the free chain ends which is of order kT per chain. At the transition this entropy loss is comparable to the energy of mixing, and we obtain $\tilde{\chi}_{\mathrm{dis}\leftrightarrow\mathrm{ripple}}\sim\delta$ (in agreement with our SCF calculations). As the incompatibility increases or the stretching decreases the decoupling of density and composition breaks down. Figure 1 illustrates the variation of the total density at intermediate stretching [15] and rather large incompatibility. In this parameter region we investigate the interplay between energy of mixing and conformational entropy via numerical SCF calculations. Additional morphologies are found to be stable and lateral and perpendicular segregation occur simultaneously.

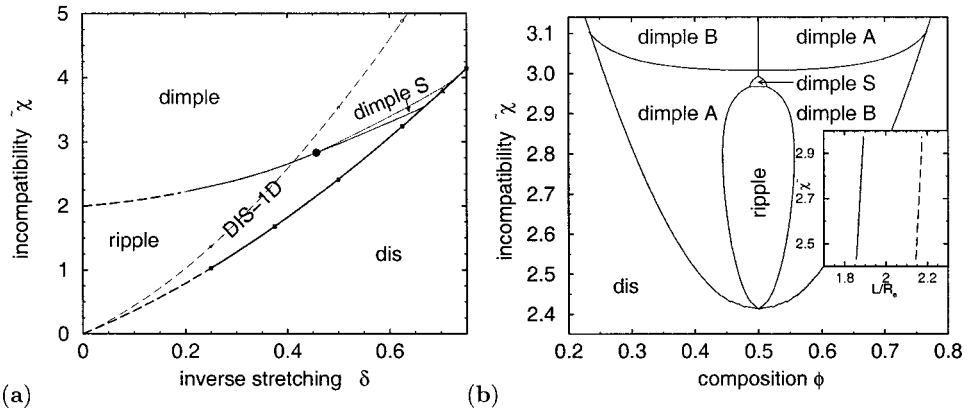

FIG. 2. (a) Phase diagram for a symmetric polymer brush ($\Phi = 1/2$): Under good solvent conditions ($\tilde{\chi} < 2$) we find a transition between a disordered (dis) and a ''ripple'' phase. In a bad solvent the disordered, the ripple, and two ''dimple'' phase are stable. The transition between the 1D phase and the disordered phase is indicated by a dashed line. It is preempted by the laterally structured phases. Our calculations are limited to $\delta > 0.23$; extrapolated phase boundaries for smaller δ are denoted by dashed lines. (b) Phase diagram for $\delta = 0.5$ as a function of the composition Φ and the incompatibility $\tilde{\chi}$. ''Dimple *A*'' and ''dimple *B*'' denote the hexagonal arrangement of *A*-rich and *B*-rich clusters, respectively. ''Dimple *S*'' refers to a checkerboard of *A*-rich and *B*-rich clusters. The inset displays the variation of the lateral unit-cell size *L* along the ''dimple''-''ripple'' phase boundary. The solid line corresponds to the ripple phase, the dashed line corresponds to the dimple phase.

First, we investigate the phase behavior for symmetric composition ($\Phi = 1/2$) as a function of stretching δ and incompatibility $\tilde{\chi}$. The relative stability of five phases is explored [16]: the disordered phase (dis) which is neither laterally nor perpendicularly segregated, the layered phase (1D), in which the symmetry between *A* and *B* is spontaneously broken and the two components segregated perpendicular to the surface, the ''ripple'' phase in which the two components segregated laterally into symmetrical cylinders, and two ''dimple'' phases. In one phase, denoted as ''dimple *S*,'' both species segregate symmetrically into clusters, which arrange like on a checkerboard. In the other phase (''dimple *A*'' or ''dimple *B*'') one of the components—*A* or *B*—segregates into clusters, which form an hexagonal lattice in the lateral direction, while the other component is less dense and fills the space between the clusters. The symmetry between *A* and *B* is broken. The (total) density profiles of the laterally structured phases are shown in Fig. 1. The size of the lateral repeat units is about $1.9R_e$ for the ripple and symmetric dimple phases and $2.2R_e$ for the hexagonal dimple phase in the range of $\tilde{\chi}$ investigated.

The phase diagram is presented in Fig. 2. Upon increasing the incompatibility, we find a second-order transition from the disordered phase to the ''ripple'' phase. As discussed above, the incompatibility $\tilde{\chi}$ at which the ''ripple'' structure forms increases linearly with δ in the limit of strong stretching $\delta \to 0$. For small values of δ and stronger incompatibility ($\tilde{\chi} > 2$, bad solvent), we encounter a transition from the ''ripple'' phase to an hexagonal ''dimple'' phase. For larger values of δ we first encounter a transition from the ''ripple'' phase to the symmetrical ''dimple *S*'' phase and at even larger incompatibilities a transition to an hexagonal ''dimple'' phase. There is a triple point at $\delta = 0.46$ and $\tilde{\chi} = 2.83$, where the ''ripple,'' the symmetrical, and the hexagonal ''dimple'' phases coexist. For $\delta > 0.25$ we find the layered structure (1D) to be unstable, however, we cannot rule out that it might become stable for larger stretching.

The phase diagram for $\delta = 1/2$ as a function of the composition Φ is presented in Fig. 2(b). At high incompatibilities or extreme compositions the majority component forms an hexagonal array of clusters. This behavior is similar to a one-component brush in a bad solvent: the brush does not collapse into a uniform dense layer, but rather forms ''dimples'' [3]. Simultaneously, there is on average a pronounced perpendicular segregation: the majority component is enriched at the grafting surface, while the minority component is expelled from the surface. At lower incompatibilities or more symmetrical composition, we again find an hexagonal ''dimple'' phase, but the minority component forms the clusters. The incompatibility $\tilde{\chi}$ is not large enough to make the majority component collapse, but it acts like a very bad solvent for the minority component. Note that there is a weak attraction between the segments of the same component, but a strong repulsion between different types of segments. Upon approaching symmetrical composition $\Phi \to 1/2$, we find transitions from the ''dimple'' phase to the ''ripple'' phase at low incompatibilities, to the symmetrical ''dimple'' phase at intermediate incompatibilities, or directly from ''dimple *A*'' to ''dimple *B*'' at $\Phi = 1/2$ and large $\tilde{\chi}$.

In summary, the irreversible end grafting of chains prevents macrophase separation in a binary brush. We have studied the self assembly into spatially structured phases within SCF theory and find a rich phase behavior including two 3D structures with truly 2D lateral periodicity: a checkerboard arrangement of *A*-rich and *B*-rich clusters (symmetric ''dimple'' phase) and an hexagonal lattice of clusters of one component (hexagonal ''dimple'' phase). In the latter phase the *AB* symmetry is spontaneously broken and it is stable for symmetric composition at high incompatibility. Experiments [17] yield evidence for the formation of lateral structure in the nanometer range and we hope they will verify our predictions.

In our calculations the solvent quality is identical for both species and the surface does not prefer either component. These additional interactions are important in experiments [1] and can be readily incorporated into our model. We anticipate an interplay between lateral and perpendicular segregation.

We assume the grafting points of the two polymer species be completely uncorrelated and homogeneous. This is a rather strong idealization, which is difficult to achieve in experimental realizations. *ACB* triblock copolymers [8] with a short middle *C* block, which chemically binds to the surface, could offer a possibility to reduce correlations.

Another exciting question is the response of the binary brush to absorbing molecules and the wetting properties of the laterally structured surface. Potentially, this class of materials offers the opportunity to tune the surface and wetting properties [1] and to tailor the interaction between different surfaces [4]. We expect our calculations to provide some guidance for controlling these materials' properties.

I have benefited from stimulating discussions with K. Binder, S. Minko, M. Stamm, and J. Rühe. Financial support was provided by the DFG under Grant No. Bi314/17 and the DAAD/PROALAR2000.

[1] A. Sidorenko *et al.*, Langmuir **15**, 8349 (1999).

[2] J. F. Marko and T. A. Witten, Phys. Rev. Lett. **66**, 1541 (1991); Macromolecules **25**, 296 (1992).

[3] P.-Y. Lai and K. Binder, J. Chem. Phys. **97**, 586 (1992).

[4] C. Singh *et al.*, Macromolecules **29**, 7637 (1996); **29**, 7559 (1996).

[5] K. Geoffrey Soga *et al.*, Macromolecules **29**, 1998 (1996).

[6] G. Brown *et al.*, Europhys. Lett. **25**, 239 (1994).

[7] P.-Y. Lai, J. Chem. Phys. **100**, 3351 (1994).

[8] M. J. Fasolka *et al.*, Phys. Rev. Lett. **79**, 3018 (1997); Macromolecules **33**, 5702 (2000).

[9] M. Boltau *et al.*, Nature (London) **391**, 877 (1998).

[10] E. Schaffer *et al.*, Nature (London) **403**, 874 (2000).

[11] A. Boker *et al.*, Macromolecules **34**, 7477 (2001).

[12] For $\tilde{\chi}>2$ the solvent is bad for the pure components, but the average segment interaction would be repulsive for $\tilde{\chi}|\Phi-1/2|<1$, if the brush was homogeneously mixed. Including third-order virial coefficients in our calculations we have verified explicitely that the qualitative features of the phase behavior remain unaltered.

[13] R. R. Netz and M. Schick, Europhys. Lett. **37**, 38 (1997); Macromolecules **31**, 5105 (1998); J. L. Goveas *et al.*, *ibid.* **30**, 5541 (1997).

[14] M. W. Matsen and M. Schick, Phys. Rev. Lett. **72**, 2660 (1994).

[15] Small values of stretching δ correspond either to a small overlap of grafted chains $\sigma R_e^2 \ll 1$ or to a solvent of marginal quality $vN^2/R_e^3 \ll 1$. In the former case correlations of the grafting points are very important in experiments, in the latter case they are not.

[16] Generally, a variety of lateral arrangements can be envisioned, however, in our calculations we need to specify the lateral symmetry. This caveat might be alleviated by recently developed SCF techniques [F. Drolet and G. H. Fredrickson, Phys. Rev. Lett. **83**, 4317 (1999); Y. Bohbot-Raviv and Z. G. Wang, *ibid.* **85**, 3428 (2000)], or possible candidates of lateral arrangements can be inferred from experiments or computer simulations.

[17] S. Minko *et al.*, Phys Rev. Lett. **88**, 035502 (2002).